Eur Biophys J (2004) 33: 435–447
DOI 10.1007/s00249-003-0376-x

ARTICLE

Elaine M. Little · Carl Holt

An equilibrium thermodynamic model of the sequestration of calcium phosphate by casein phosphopeptides

Received: 26 August 2003 / Revised: 3 November 2003/Accepted: 6 November 2003 / Published online: 20 January 2004

Abstract Sequestration of calcium phosphate by caseins occurs in the Golgi region of mammary secretory cells during lactation, where it helps to prevent calcification of the gland and to deliver high concentrations of calcium and phosphate to the neonate in the form of milk. Calcium phosphate nanoclusters are formed when a core of amorphous calcium phosphate is sequestered within a shell of casein or casein phosphopeptides. The nanoclusters can form spontaneously from a supersaturated solution or by dispersion of a precipitate of calcium phosphate, demonstrating that they are thermodynamically stable complexes. The average size and chemical composition of the complexes are largely independent of the solution conditions (pH, temperature, peptide concentration, salt composition and rate of reaction) under which they form. Larger, metastable, colloidal particles can form if there is not enough of the phosphopeptide to sequester all the calcium phosphate, or, transiently, if the salt and peptide solutions are mixed together without sufficient care. A thermodynamic model of the sequestration process is presented which makes use of an invariant ion activity product observed in nanocluster-containing solutions. In any given solution that has thermodynamic stability, the extent of the sequestration reaction can be calculated from the empirical formula of the nanoclusters using the criterion that the solution should have the equilibrium value of the invariant ion activity product. Other members of the paralogous group of secretory calcium-binding phosphoproteins to which caseins belong may also be able to sequester calcium phosphate in biological fluids such as saliva and in the extracellular matrix of mineralizing tissues.

E. M. Little · C. Holt (✉)
Hannah Research Institute, Ayr, KA6 5HL, UK
E-mail: c.holt@hannah.ac.uk
Tel.: +44-1292-674084
Fax: +44-1292-674003

Keywords Calcium phosphate · Casein · Phosphopeptide · Secretory calcium-binding phosphoprotein

Abbreviations α-PP: α_{s1}-casein 5P (f59–79) · β-PP: β-casein 4P (f1–25) · ACP: amorphous calcium phosphate · Cit: citrate · CPN: calcium phosphate nanocluster · CPP: commercial phosphopeptide · IAP: ion activity product · MWCO: molecular weight cut-off · PP: phosphopeptide · SAXS: small-angle X-ray scattering · SCPP: secretory calcium-binding phosphoprotein · UF: ultrafiltrate

Introduction

The caseins of milk, certain salivary proteins and some extracellular matrix proteins of bone, dentine and enamel constitute the known members of a paralogous group of secretory calcium-binding phosphoproteins (SCPPs) (Rijnkels 2002; Fisher and Fedarko 2003; Kawasaki and Weiss 2003). Like most other members of the paralogous group, caseins have a natively unfolded, or rheomorphic, conformation (Holt and Sawyer 1993; Syme et al. 2002; Tompa 2002) and most have one or more multiply phosphorylated short sequences (phosphate centres) through which they can interact with calcium phosphate. Although the functions of most members of the paralogous group are poorly understood, that of caseins is not. These proteins have the ability to sequester calcium phosphate as nanometre-sized clusters of ions surrounded by a shell of protein.

Holt et al. (1996) showed that nanometre-sized complexes called calcium phosphate nanoclusters (CPN) form spontaneously from a solution of salts at milk concentrations, containing also the hydrophilic, 25-residue, N-terminal, tryptic phosphopeptide from β-casein (β-PP) at a concentration of 1.6 mM. The structure of the nanocluster was determined (Holt et al. 1998) by sedimentation equilibrium in combina-

tion with X-ray and contrast-matched neutron scattering methods and shown to consist of a core of calcium phosphate with a mass of 61 kDa and radius 2.4 nm surrounded by a shell of about 50 peptides having an outer radius of 4 nm. In milk, nanometre-sized clusters of calcium phosphate are sequestered by the caseins in much larger colloidal particles called casein micelles (De Kruif and Holt 2003). A typical micelle of about 100 nm radius contains about 800 calcium phosphate nanoclusters in a disordered array (Holt et al. 2003).

Casein was once described as a random coil protein having only a nutritional function (McMeekin 1971). It is becoming increasingly apparent, however, that natively unfolded proteins can have more specific biological functions even though they have no fixed conformation (Dunker et al. 2002; Dyson and Wright 2002). Some natively unfolded proteins have a preponderance of poly-L-proline-II secondary structure which gives the polypeptide the character of a stiff, worm-like chain (Petrescu et al. 1998), or as Holt and Sawyer (1993) termed it, a rheomorphic conformation. Indeed, we have proposed that the casein micelle fulfils the vital biological function of protecting the mammary gland against calcification by sequestering the high concentrations of calcium phosphate in the form of nanoclusters (Holt and Sawyer 1993; DeKruif and Holt 2003). The ability to do so with the required speed is facilitated by the flexible conformation. The nanoclusters were envisaged to be in a metastable state of arrested precipitation because of their interaction with casein and it was for this reason that the gentle and homogeneous method of raising the pH by hydrolysis of urea to ammonia was employed to make the nanocluster particles in the laboratory (Holt et al. 1996, 1998). Subsequently it was found that the nanoclusters can also be formed by the addition of phosphopeptides to a pre-formed amorphous calcium phosphate (ACP) precipitate (Holt 2000), demonstrating that the complex is more thermodynamically stable than the precipitate.

It is shown here that thermodynamically stable nanoclusters can be made using phosphopeptides derived from β- or α_{s1}-casein or a commercial mixture of casein tryptic phosphopeptides. An equilibrium thermodynamic model of the formation of the nanoclusters is described which is consistent with what we know of their structure and from which a stability condition is derived for the formation of the nanoclusters. The work goes some way towards understanding the remarkable ability of caseins to sequester calcium phosphate.

Materials and methods

Analytical methods and ultrafiltration

Ca and P_i were determined by the methods of Connerty and Briggs (1966) and Allen (1940), respectively. Mg was measured using the Calmagite test kit 595 A (Sigma-Aldrich, Poole, UK) and citrate (Cit) using the UV test kit of Boehringer-Mannheim. The free calcium ion concentration was measured with a model 93-3209 selective ion electrode (Russel pH, Auchtermuchty, UK) calibrated with solutions of matched ionic strength. Ultrafiltration was carried out in a stirred cell at 100 kPa through a PM10 membrane of 10,000 molecular weight cut-off (MWCO) (Millipore, Bedford, Mass., USA). The CPN solution ultrafiltrates (UFs) prepared in this way were essentially free of phosphopeptide (PP).

Preparation of the phosphopeptides

The isolation and purification of the β-PP has been described previously (Holt et al. 1996 and references cited therein). The α_{s1}-casein (α-PP) was prepared by a very similar method involving tryptic cleavage of the protein and isolation of the phosphopeptides as Ba salts, followed by chromatography of the phosphopeptide mixture on a hydroxyapatite column (1.5×30 cm, Biogel HTP, BioRad) at a flow rate of 1.6 mL min^{-1}. The freeze-dried tryptic digest was loaded on the column in 10 mM P_i, pH 6.8, containing 100 mM KCl. Elution by a phosphate salt gradient (1100 mL of 10–300 mM) yielded four fractions that were, in order of elution, α_{s1}-CN 1-P (f104–119), α_{s1}-CN 2-P (f43–58), unidentified and α_{s1}-CN 5-P (f59–79). Fraction 4 was separated on a Q-Sepharose High Performance column (Amersham Bioscience, Little Chalfont, UK) into two approximately equal peaks, 4a and 4b. Analysis by MS and MS^2 showed that the mass of 4a was 18 Da less than 4b and it was less negatively charged. Other evidence from the mass spectrum suggested that the N-terminal Gln had partially formed a cyclic pyroglutamate. The fractions 1, 2, 4a and 4b were tested for their ability to form nanoclusters under standard conditions (buffer A, pH 6.7, 5 mg mL^{-1}) [buffer A = 22 mM $Ca(NO_3)_2$, 5 mM $Mg(NO_3)_2$, 17.5 mM KH_2PO_4, 2.5 mM K_2HPO_4, 36 mM KNO_3, 1.5 mM NaN_3]: whereas 1 and 2 failed to inhibit precipitation, fractions 4a and 4b behaved very similarly to the β-PP and formed nanoclusters.

The commercial phosphopeptide (CPP) mixture was obtained from MD Foods, Denmark (now Arla) as a sodium salt. The preparation, composition and some properties of the peptide mixture have been described by Ellegård et al. (1999).

Small-angle X-ray scattering

SAXS measurements were performed on station 2.1 at the CLRC Daresbury Laboratory over the period 1994–2002 using the quadrant ion detector and camera lengths of 1.25–6.25 m. Scattered intensity was normalized against the transmitted intensity, as measured by a diode on the beam stop. Calibration of the station and some operational details have been described previously (Towns-Andrews et al. 1989). Samples were held in a brass cell with mica windows having an optical path length of 1 mm. The cell was normally thermostatted at 20 °C, but one sample was studied at temperatures in the range 5–80 °C.

Differential scanning calorimetry

The specific heat change during the heating stages was recorded by microcalorimetry as described previously (Qi et al. 1997). In this experiment a CPN solution (5 mg β-PP mL^{-1} in buffer B) [buffer B = 30 mM $Ca(NO_3)_2$, 5 mM $Mg(NO_3)_2$, 20 mM KH_2PO_4, 26 mM KNO_3, 1.5 mM NaN_3] was heated from 4 to 100 °C, cooled to 4 °C and re-heated to 100 °C.

Binding isotherms for β-PP

The binding of Ca^{2+} to β-PP was measured as a function of pH in the range 5.5–8.0. The peptide was dissolved in 10 mM imidazole buffer with 60 mM KNO_3 at a concentration of 1.6 mM. Sequential additions of a stock 100 mM solution of $CaCl_2$ were made to the phosphopeptide solution and the free calcium ion concentration measured. The concentration of bound Ca was obtained as the difference between the total Ca and free concentrations after each addition. Figure 1 shows that the binding decreases as the pH decreases because of the competing equilibria between Ca^{2+} and H^+ for the phosphate moiety of the phosphorylated residues. Accordingly, the maximum binding was about 4 mol Ca (mol β-PP)$^{-1}$. The extent of binding is consistent with the apparent Ca^{2+} binding constants for the phosphopeptide reported by Baumy et al. (1989) at pH 3–8. Polynomial equations, $\bar{\nu}_{Ca} = \sum_{i=0}^{3} a_i[Ca^{2+}]^i$, were fitted to the binding isotherms. The regression coefficients, a_i, were themselves fitted to a quadratic function in pH so that the isotherm at any intermediate pH could be computed by interpolation.

Preparation of calcium phosphate nanoclusters from a calcium phosphate precipitate

In these experiments, attempts were made to form CPNs by the "reverse" reaction. Earlier qualitative observations (Holt 2000) indicated that a freshly made calcium phosphate precipitate could be redispersed at neutral pH by addition of a sufficient concentration of CPP. Likewise, a standard nanocluster solution taken to pH > 8 formed a precipitate over time, but on reducing the pH to 6.7 the precipitate spontaneously redispersed to form a clear solution.

In the present experiments, a systematic examination was made of the effect of CPP or β-PP concentration on the redispersion process over a period of 12 months. A fresh calcium phosphate precipitate was prepared by raising the pH from 5.5 to 6.7 of a solution containing 30 mM $Ca(NO_3)_2$, 4 mM $Mg(NO_3)_2$, 20 mM P_i (K_2HPO_4 and KH_2PO_4), 10 mM K_3Cit, 26 mM KNO_3 and 1.5 mM NaN_3. Approximately 30 min after reaching the pH and the formation of a flocculent precipitate of ACP, the solid phosphopeptide was added to a final concentration of 0, 2, 5, 10 or 15 mg CPP mL^{-1}, and allowed to dissolve. In a separate but similar experiment, β-PP was substituted for the CPP. The solutions were allowed to stand in sealed bottles at room temperature with a periodic inversion of the container to remix any condensation. The bottles were photographed at regular intervals to provide a record of the change in appearance of the contents and the pH recorded. After approximately 6 months and 12 months, samples were removed from bottles that appeared to be free of precipitate for size measurement by SAXS.

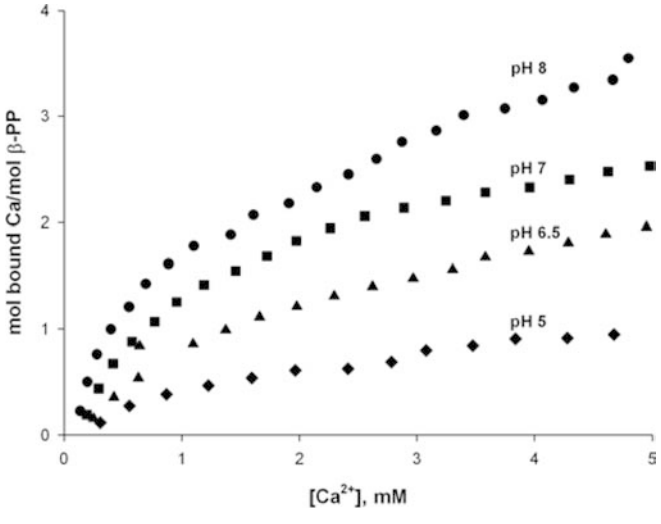

Fig. 1 Calcium binding isotherms of β-PP as a function of pH

Preparation of calcium phosphate nanoclusters from solution

Nanoclusters were first prepared by the "forward" reaction by raising the pH of a solution containing Ca and P_i homogeneously with urea and urease to generate the strong base ammonia. With suitable salt concentrations, but without the phosphopeptide, a precipitate of calcium phosphate formed after the solution became supersaturated. If the concentration of phosphopeptide is large enough, however, a complex is formed between the calcium phosphate and the peptide and no precipitate or colloidal particles formed. It also proved possible to prepare thermodynamically stable nanoclusters by a simpler mixing process (Holt 2000), although some colloidal particles were sometimes formed transiently. The mixing was done slowly, and sometimes with a specific sequence of salt additions, to avoid local excess concentrations and precipitation of calcium phosphate, but it was possible to achieve complete mixing with only a slight opalescence in the resulting solution. Within a few days or weeks, the initial opalescence decreased to give a solution of the nanocluster complexes with few colloidal particles.

It was reported previously that some variation in the size of nanoclusters occurred even with the urea/urease method, according to the rate at which the pH was raised (Holt et al. 1996). Further work has shown, however, that by the following day the nanoclusters all had the same size, irrespective of the rate of pH increase. The urea/urease method remains the technique of choice for preparing the most homogeneous samples and is the one used here. Standard nanoclusters were prepared using buffer A or buffer B with 1.6 mM β-PP at a pH of 6.7–6.8.

Variation of pH

Samples were prepared by adjusting the urea concentration (0.67–30 mM) to give a final pH in the range 5.8–8.0. The initial solution, buffer A, contained either 1.6 mM β-PP or α-PP or 10 mg mL^{-1} CPP. A further series of measurements was performed on buffer B solutions containing 5 or 10 mg CPP mL^{-1}. Buffer B gave very similar free Ca^{2+} ion concentrations to the buffer A mixture at the same pH, with the advantage that it is more similar to the composition of cows' milk. After the pH had stabilized, some of the samples were ultrafiltered through a 10,000 MWCO membrane at 100 kPa and the concentrations of the multivalent components (Ca, Mg, P_i, Cit) determined on the UF. Similar samples were also prepared for the measurement of nanocluster size by SAXS.

Variation of peptide concentration

The effect of β-PP concentration (1.6–6.4 mM) on the size of the nanoclusters at pH 6.7 was determined using buffers A and B. The effect of CPP concentration (5–20 mg mL^{-1}) on the size of the nanoclusters was also determined using buffer B.

Variation of Mg and Cit concentrations

The effect of Mg concentration (0–5 mM) on the size of the nanoclusters at pH 6.7 was determined by varying its concentration in buffer A containing 1.6 mM β-PP. The effect of Cit concentration (0–10 mM) on the size of the nanoclusters at pH 6.7 was determined using buffer A and buffer B or mixtures of the two, each containing 1.6 mM β-PP.

Theory

Thermodynamic model

Consider the equilibria in a Mg-free buffer A containing enough β-PP to form the CPN with an empirical formula:

$$Ca_{R_{Ca}}H_{R_H}(P_i)_{R_P}(H_2O)_{R_W}\beta\text{-PP} \tag{1}$$

where R_X is the molar ratio of component X to the β-PP. The phosphopeptide can be represented as an electroneutral Gibbs component with 15 exchangeable protons, $H_{15}\beta$-PP. The empirical formula for the CPN can be written as an acidic calcium phosphate and a calcium phosphopeptide:

$$\left[Ca_{\frac{3}{2+y}R_P}(HPO_4)_{\frac{3y}{2+y}R_P}(PO_4)_{\frac{2-2y}{2+y}R_P}(H_2O)_{R_W}\right][Ca_mH_n\beta\text{-PP}] \tag{2}$$

where $3y/(2+y)$ is the mole fraction of P_i in the di-anionic form:

$$\begin{aligned} m &= (R_{Ca} - 32 + yR_P) \\ n &= 15 - 2m \end{aligned} \tag{3}$$

Using the electroneutral Gibbs components, the sequestration process can be divided into two parts corresponding to the formation of the core of calcium phosphate:

$$\begin{aligned} &\left(\frac{3}{2+y}R_P\right)Ca(OH)_2 + R_PH_3PO_4 \\ &\quad\rightleftharpoons \left[Ca_{\frac{3}{2+y}R_P}(HPO_4)_{\frac{3y}{2+y}R_P}(PO_4)_{\frac{2-2y}{2+y}R_P}(H_2O)_{R_W}\right] \\ &\qquad + \left(\frac{6}{2+y}R_P - R_W\right)H_2O \end{aligned} \tag{4}$$

and the sequestration of the core by a shell of the calcium phosphopeptide to form the complete nanocluster complex:

$$\begin{aligned} &\left[Ca_{\frac{3}{2+y}R_P}(HPO_4)_{\frac{3y}{2+y}R_P}(PO_4)_{\frac{2-2y}{2+y}R_P}(H_2O)_{R_W}\right][Ca_mH_{(15-2m)}\beta\text{-PP}] \\ &\quad + 2mH_2O \end{aligned} \tag{5}$$

The Gibbs free energy of forming the CPN is divided into the free energy of forming the core (ΔG_{core}) and the free energy of sequestering the core in the shell (ΔG_{seq}):

$$\Delta G_{CPN} = \Delta G_{core} + \Delta G_{seq} \tag{6}$$

It is convenient to express the free energy per mole of Ca in the core. Applying the Gibbs–Duhem relation to Eq. (4) and expanding the chemical potentials in the usual way yields:

$$\Delta G_{core} = \Delta G^{\circ}_{core} + RT\ln a_{core} - RT\ln(IAP) \tag{7}$$

$$\Delta G^{\circ}_{core} = \mu^{\circ}_{core} - \mu^{\circ}_{Ca^{2+}} - y\mu^{\circ}_{HPO_4^{2-}} - \left(\frac{2-2y}{3}\right)\mu^{\circ}_{PO_4^{3-}} \tag{8}$$

$$IAP = \{Ca^{2+}\}\{HPO_4^{2-}\}^y\{PO_4^{3-}\}^{(2-2y)/3} \tag{9}$$

where μ°_X and $\{X\}$ are the chemical potential of X in its standard state and the activity of X, respectively, and a_{core} is the activity of the calcium phosphate in the core. Nanocluster complexes containing small proportions of Mg and Cit can be formed from solutions such as buffer B and an empirical formula and ion activity product (IAP) formulated by analogy with Eqs. (1) and (9), respectively.

In the precipitation of a bulk phase with the same chemical composition as the CPN core:

$$\Delta G_{bulk} = \Delta G^{\circ}_{bulk} - RT\ln\left(\frac{IAP}{a_{bulk}}\right) \tag{10}$$

$$\Delta G^{\circ}_{bulk} = \mu^{\circ}_{bulk} - \mu^{\circ}_{Ca^{2+}} - y\mu^{\circ}_{HPO_4^{2-}} - \left(\frac{2-2y}{3}\right)\mu^{\circ}_{PO_4^{3-}} \tag{11}$$

At equilibrium with the saturated solution, $\Delta G_{bulk} = 0$ and $a_{bulk} = 1$, by definition for a pure substance, so:

$$\begin{aligned} \Delta G^{\circ}_{bulk} &= RT\ln K_{Sp} \\ K_{Sp} &= IAP \end{aligned} \tag{12}$$

where K_{Sp} is the solubility product.

ΔG_{core} is likely to be less negative than that of the bulk phase because of the additional surface energy. The Kelvin equation for the activity of a substance with a molar volume $\bar{V}$ in the form of a sphere of radius R_{core} and having an interfacial tension γ_S may be expressed as:

$$RT\ln\left(\frac{a_{core}}{a_{bulk}}\right) = \frac{2\bar{V}\gamma_S}{R_{core}} \tag{13}$$

Typically, we might expect the activity of a nanometre-sized cluster to be about an order of magnitude greater than that in the of bulk phase because of the high surface energy of ionic solids. Replacement of the high-energy interface with a low-energy peptide interface will reduce the activity ratio in Eq. (13). It is shown below that the average size of nanoclusters formed under a wide range of solution conditions is constant, suggesting that a_{core} is constant and hence:

$$\Delta G^{\circ}_{core} = RT\ln(IAP) - RT\ln a_{core} = RT\ln K'_S \tag{14}$$

The additional free energy of forming the core compared to the bulk phase is more than compensated for by the free energy of sequestration of the core within the shell. The free energy of sequestration may be considered to be derived from a reduction in the interfacial energy and the formation of the shell itself, both of which are held to be constant for a given core radius. Hence, for the spontaneous formation of the CPN:

$$\begin{aligned} &\Delta G^{\circ}_{seq} = -RT\ln K_{seq} \\ &\Delta G^{\circ}_{CPN} = RT\ln\left(K_S/K_{seq}\right) = RT\ln K \\ &\Delta G^{\circ}_{CPN} < \Delta G^{\circ}_{bulk} < \Delta G^{\circ}_{core} \\ &\Delta G^{\circ}_{seq} < \Delta G^{\circ}_{bulk} - \Delta G^{\circ}_{core} \end{aligned} \tag{15}$$

Although the magnitudes of K_S and K'_S will differ as a result of the sequestration reaction, it seems reasonable to assume that an invariant IAP will apply to the nanocluster solution since the small ions are in dynamic equilibrium (Holt et al. 1996). The form of the IAP will correspond to the empirical chemical formula of the core after sequestration, as expressed by Eq. (9). The equilibrium value of the IAP can be used to calculate all the chemical species, including the CPN.

Calculation of the chemical species

The validity of the thermodynamic model was tested by comparing the calculated and experimental composition of UFs prepared from nanocluster solutions. All the ionic species that are fully permeable establish an electrochemical equilibrium across the membrane and the ion activities can be determined from a suitable model of the multiple ion equilibria (Holt et al. 1981). The values of y and K_S are found by determining an invariant form of the IAP, and its value, from the analysis of a wide range of UF compositions.

In a nanocluster solution, the concentration of the CPN is fully specified if the extent of reaction of the phosphopeptide, α, is known and the extent of reaction is determined when the IAP is equal to K_S. Thus the calculation of the chemical species uses an extension to the model of the ion equilibria in the UF to allow for the binding of ions to the free phosphopeptide and the formation of the CPN complexes.

The binding of calcium ions to the free peptide is calculated from binding isotherms determined at several pH values and, by interpolation, adjusted to the experimental pH. It is assumed that when both magnesium and calcium ions are present they are bound in proportion to their free ion activities. Thus, the non-permeating or complexed concentrations are calculated from:

$$[\mathrm{Ca}]_c = [\mathrm{PP}](R_{\mathrm{Ca}}\alpha + (1-\alpha)\bar{\nu}_{\mathrm{Ca}}(\mathrm{pH}, \{\mathrm{Ca}^{2+}\}, \{\mathrm{Mg}^{2+}\})) \quad (16)$$

$$[\mathrm{Mg}]_c = [\mathrm{PP}](R_{\mathrm{Mg}}\alpha + (1-\alpha)\bar{\nu}_{\mathrm{Mg}}(\mathrm{pH}, \{\mathrm{Ca}^{2+}\}, \{\mathrm{Mg}^{2+}\})) \quad (17)$$

$$[\mathrm{H}]_c = [\mathrm{PP}](R_{\mathrm{H}}\alpha + (1-\alpha)\bar{\nu}_{\mathrm{H}}(\mathrm{pH}, \{\mathrm{Ca}^{2+}\}, \{\mathrm{Mg}^{2+}\})) \quad (18)$$

where $\bar{\nu}_{\mathrm{Ca}}$ and $\bar{\nu}_{\mathrm{Mg}}$ are the average number of bound Ca and Mg ions per mole of phosphopeptide, respectively.

For the anions Cit and P_i, only a single term is needed since they are not thought to bind to caseins other than through the CPN:

$$[\mathrm{Cit}]_c = [\mathrm{PP}]R_{\mathrm{Cit}}\alpha \quad (19)$$

$$[\mathrm{P_i}]_c = [\mathrm{PP}]R_{\mathrm{P}}\alpha \quad (20)$$

Other ion equilibria are calculated as described previously (Holt et al. 1981).

Structural model

In a SAXS experiment, the normalized scattered intensity $I(Q)$ is measured. For a dispersion of isotropic, monodisperse particles, $I(Q)$ is related to the inter-particle structure factor, $S(Q)$, and the particle scattering factor, $P(Q)$, by (Feigin and Svergun 1987):

$$I(Q) \propto \frac{NM}{V}P(Q)S(Q) \quad (21)$$

where N is the number of particles of mass M in a volume V. The scattering wave vector, Q, is:

$$Q = \frac{4\pi}{\lambda}\sin\theta \quad (22)$$

where 2θ is the scattering angle and λ is the wavelength of the X-rays.

The proportionality constant in Eq. (21) depends on the difference between the scattering densities of the particle and the solvent. For a core of electron density ρ_{core}, surrounded by a shell of electron density ρ_{shell} and outer radius R, the particle scattering factor is:

$$P(Q) = \left[\frac{(\rho_{\mathrm{shell}}-\rho_{\mathrm{core}})R^3 j(QR)/QR + (\rho_{\mathrm{core}}-\rho_s)R_{\mathrm{core}}^3 j(QR_{\mathrm{core}})/QR_{\mathrm{core}}}{(\rho_{\mathrm{shell}}-\rho_{\mathrm{core}})R^3 + (\rho_{\mathrm{core}}-\rho_s)R_{\mathrm{core}}^3}\right]^2 \quad (23)$$

where ρ_s is the solvent electron density and:

$$j(x) = 3(x^{-2}\sin x - x^{-1}\cos x) \quad (24)$$

Equation (23) is approximated by $P(Q) = \exp(-Q^2R_g^2/3)$ for $QR_g < 1$. Hence, at infinite dilution, where $S(Q) = 1$ for discrete scatterers, a Guinier plot of log$I$ versus Q^2 gives the radius of gyration, R_g, from the initial slope. At finite concentrations, an apparent R_g is obtained that can be affected by the non-ideality of the solution and inter-particle scattering. The radius of gyration of the core-shell nanocluster is given by:

$$R_g^2 = \frac{3}{5}\left(\frac{(\rho_{\mathrm{core}}-\rho_s)R_{\mathrm{core}}^5 + (\rho_{\mathrm{shell}}-\rho_{\mathrm{core}})R^5}{(\rho_{\mathrm{core}}-\rho_s)R_{\mathrm{core}}^3 + (\rho_{\mathrm{shell}}-\rho_{\mathrm{core}})R^3}\right) \quad (25)$$

It is assumed that there is some polydispersity in R_{core} which follows a log-normal distribution:

$$\psi(R_{\mathrm{core}}) = \frac{1}{2\sqrt{2}\pi R_{\mathrm{core}}\beta}exp\left\{-\frac{ln(R_{\mathrm{core}}/R_o)}{\beta\sqrt{2}}\right\}^2 \quad (26)$$

where R_o is the radius of the core at the maximum, $\psi(R_{\mathrm{core}})\mathrm{d}R_{\mathrm{core}}$ is proportional to the number of particles between R_{core} and $(R_{\mathrm{core}+\mathrm{d}R\mathrm{core}})$ and β is related to the relative standard deviation in a normal or Gaussian distribution (σ_{rel}) by:

$$\sigma_{\mathrm{rel}}^2 = \exp(\beta^2) - 1 \quad (27)$$

The average particle scattering factor is then:

$$\bar{P}(Q) = \frac{\int_0^\infty \psi(R_{\mathrm{core}})M(R_{\mathrm{core}})P(Q,R_{\mathrm{core}})\mathrm{d}R_{\mathrm{core}}}{\int_0^\infty \psi(R_{\mathrm{core}})M(R_{\mathrm{core}})\mathrm{d}R_{\mathrm{core}}} \quad (28)$$

According to the model, the core mass is proportional to R_{core}^3, whereas the shell mass is proportional to R_{core}^2. Taking $m_{\mathrm{core}=61\ \mathrm{kDa}}$, $m_{\mathrm{shell}} = 136$ kDa and $R_{\mathrm{core}} = 2.39$ nm (the standard nanoclusters prepared with β-PP and characterized by neutron scattering contrast variation), the proportionality constants can be evaluated, giving:

$$M(R_{\mathrm{core}}) = 4.46R_{\mathrm{core}}^3 + 8.68M_{\mathrm{pep}}R_{\mathrm{core}}^2 \quad (29)$$

for the masses in kDa and the radius in nm.

The model is completed by an expression for the constant shell thickness, $t = R - R_{\mathrm{core}}$, consistent with the assumption that the shell mass density is a constant and hence that the shell mass is proportional to its volume. The value of t, in nm, is obtained as the single real root of:

$$t^3 + 7.17t^2 + 17.13t - 19.06M_{\mathrm{pep}} = 0 \quad (30)$$

where M_{pep} is the peptide mass in kDa. Equation (30) yields thickness values of 1.65 and 1.44 nm for shells of the β-PP and α-PP, respectively.

Results and discussion

Effect of temperature

It was observed by SAXS that the size of the standard nanoclusters was independent of T throughout the measured range of $5 \le T \le 80$ °C. Nevertheless, the intensity of the excess scatter from the nanoclusters did increase with temperature and returned to its original value on cooling. This was one of the first observations to suggest that the CPN was not a kinetically stabilized particle but a complex with thermodynamic stability. Clearly, while the number of nanoclusters increased with temperature, the nanoclusters that formed were always the same size, whatever the temperature.

A DSC curve of a nanocluster solution is shown in Fig. 2. The smooth change in specific heat, ΔC_p, with T shows no evidence of a cooperative transition such as a phase change. Moreover, a re-scan of the same solution immediately after cooling gave a curve that was closely similar to the original (Fig. 2), demonstrating that the specific heat changes were fully reversible.

Effect of peptide concentration

It was shown previously that in a milk-like solution of salts containing 1.6 mM β-PP a nanocluster solution was formed, but, at a lower concentration of 1 mM, a precipitate formed almost immediately. At intermediate concentrations, there was a tendency to form a mixture of precipitated calcium phosphate and colloidal particles with limited stability. Figure 3 shows that at

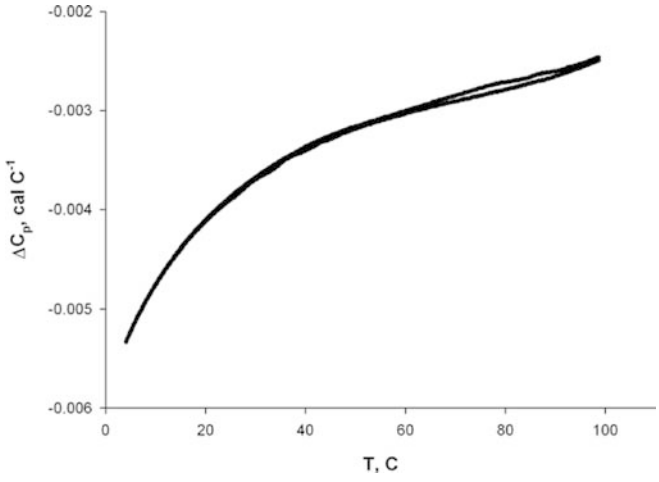

Fig. 2 Differential scanning calorimetry of a nanocluster solution (5 mg β-PP mL^{-1}) in buffer B at pH 6.77. Consecutive scans of the same solution demonstrate the absence of a cooperative phase transition and the complete reversibility of the solution in the temperature range 4–100 °C

concentrations above 5 mg mL^{-1} (1.6 mM), the size of the nanoclusters hardly changed. Indeed, the small apparent change in R_g may be due only to the non-ideality of the solution or secondary scattering. Also shown in Fig. 3a is the effect of concentration on the size of the CPP nanoclusters. At or above 10 mg mL^{-1}, the nanoclusters formed with the peptide mixture are also almost constant in size but are larger, by about 1 nm. In contrast, at 5 mg mL^{-1}, the CPP solution forms much larger particles. The reason may be that some of the peptides in the CPP are not as highly phosphorylated as the β-PP and hence the weight concentration needed for nanocluster formation is higher.

Effect of salt concentrations

The apparent radii of gyration of nanoclusters were independent of the concentrations of either Mg or Cit, as shown in Fig. 3b and Fig. 3c, suggesting that these

Fig. 3 (**a**) Effect of peptide concentration on the apparent radius of gyration of calcium phosphate nanoclusters formed with β-PP (*circles*) or CPP (*squares*). (**b**) Effect of Cit concentration on the apparent radius of gyration of CPN. (**c**) Effect of Mg concentration on the radius of gyration of CPN. (**d**) Effect of maturation time on the radius of gyration of CPN formed from β-PP (*circles*) or CPP (*squares*)

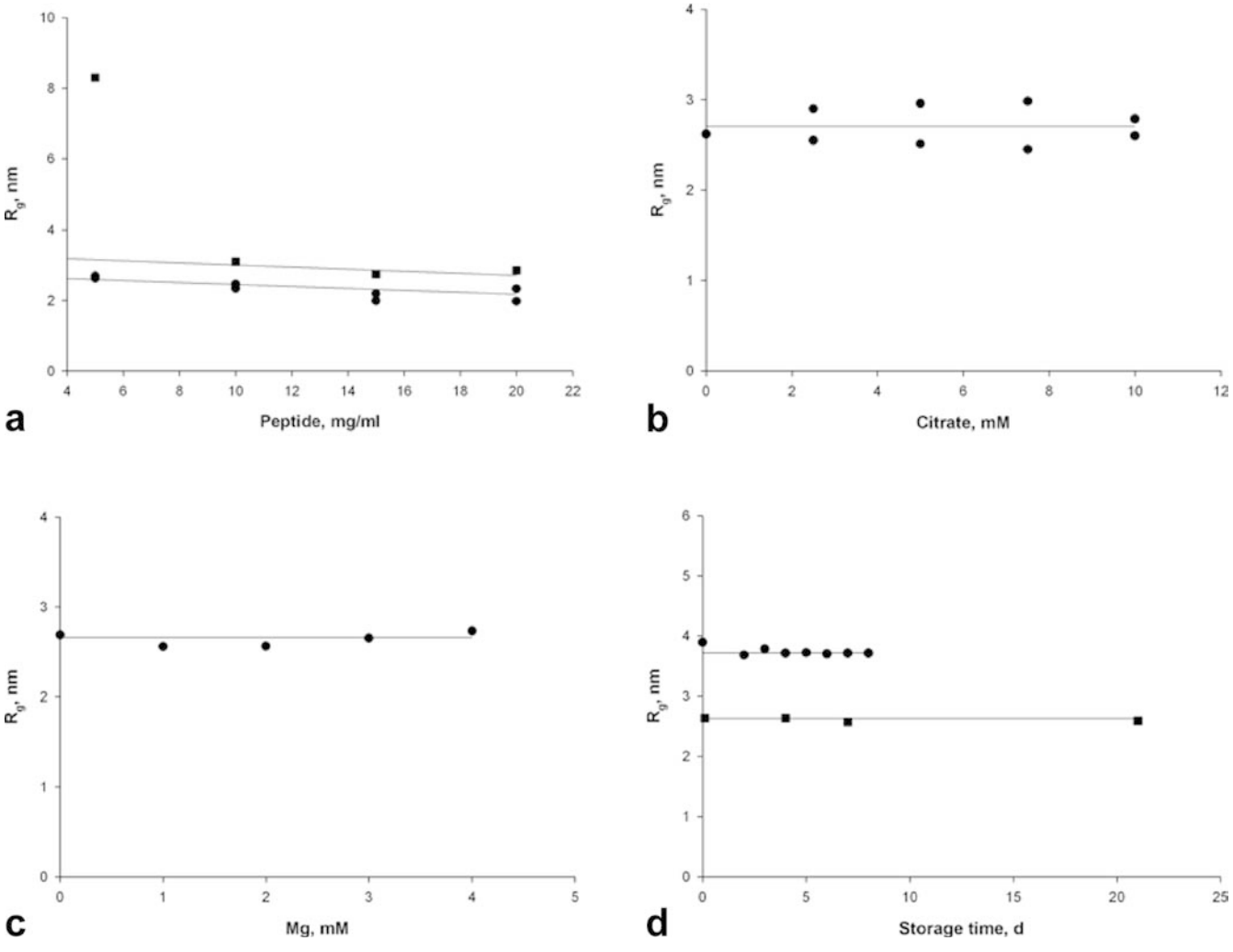

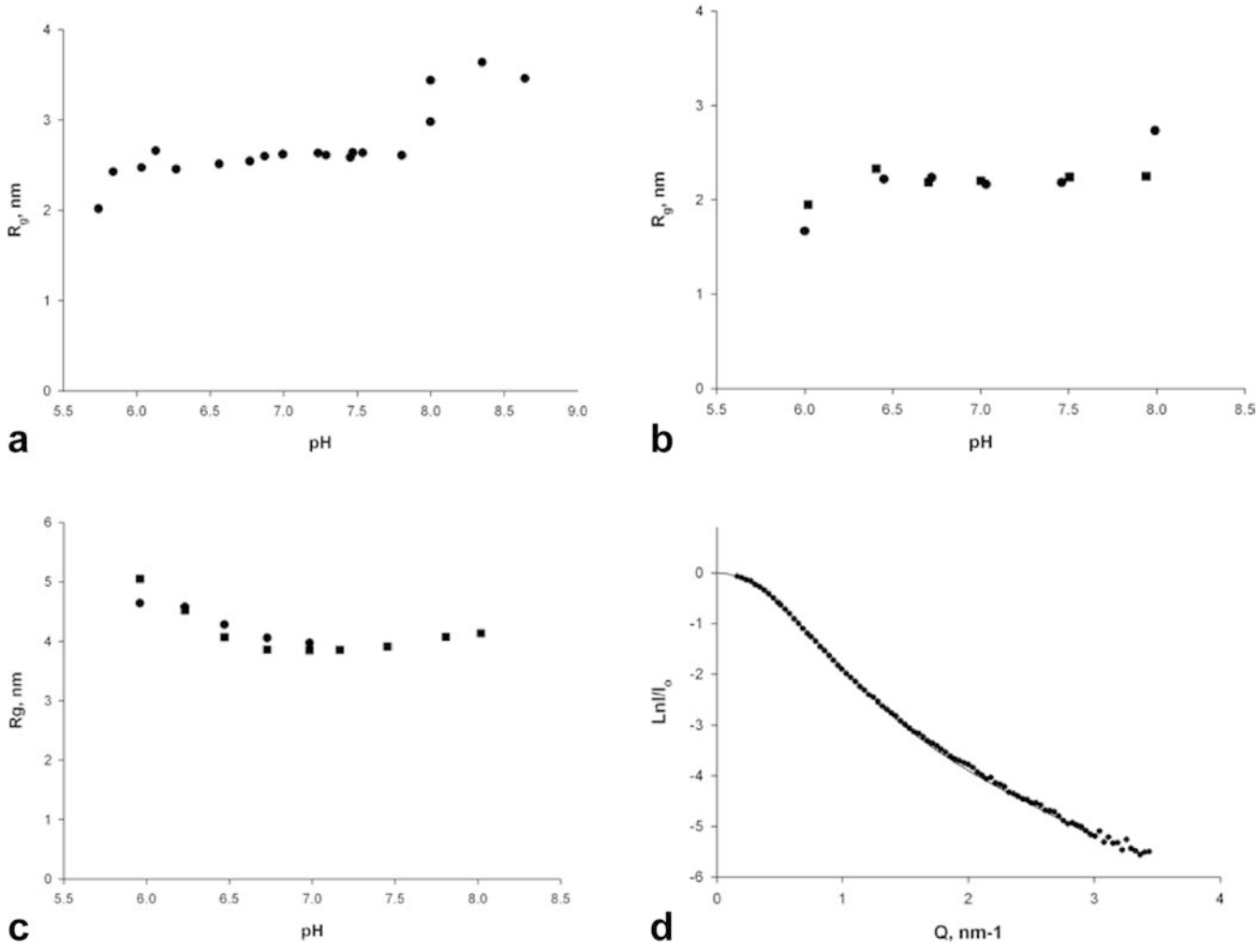

Fig. 4 Effect of pH on the X-ray scattering of nanoclusters: (**a**) β-PP; (**b**) α-PP (results for fractions 4a and 4b were indistinguishable); (**c**) CPP in buffer A (*circles*) or B (*squares*). (**d**) SAXS of β-PP nanoclusters in buffer A, pH 6.7, and fitted curve calculated from Eq. (28) with $R_o = 1.08$ nm and $\beta = 0.41$

ions did not strongly affect the formation of the complex. This is supported by the chemical evidence that they are present in the complex only as minor components.

Effect of maturation time

Nanoclusters were prepared with either β-PP or CPP up to 20 days before the measurement of their size by SAXS. As shown in Fig. 3d, the size of the complexes did not change over this timescale. Indeed, observations of nanocluster solutions over several years indicate that they are indefinitely stable.

Effect of pH on the size of nanoclusters

The variation in the apparent radius of gyration of the β-PP and α-PP nanoclusters with pH is shown in Fig. 4a and Fig. 4b, respectively. The clusters were detectable by a small increase in the intensity of scatter at about pH > 5.8. Between pH 6 and about 7.5 the size remained constant, although the intensity increased considerably, so essentially only the number of nanoclusters changed. In this range the R_g values of the β-PP and α-PP nanoclusters were 2.55 ± 0.08 and 2.23 ± 0.05 nm, respectively. Above pH 8, the measurements became less reproducible and time dependent, resulting in the slow formation of colloidal particles or a calcium phosphate precipitate. When the pH was returned to neutral, however, the precipitate or colloid spontaneously redispersed.

The dependence on pH of the CPP nanoclusters was found to be more complicated (Fig. 4c), since there was a shallow minimum rather than an extended pH range over which a constant size of cluster was observed. A minimum size at about pH 7 of 3.8 nm was observed. Moreover, at any given pH, the sizes determined in buffers A and B were very similar. Presumably, the minimum arises because the relative activities of the various peptides in the mixture change with pH and the size of the nanoclusters depends to some extent on the nature of the peptide in the shell.

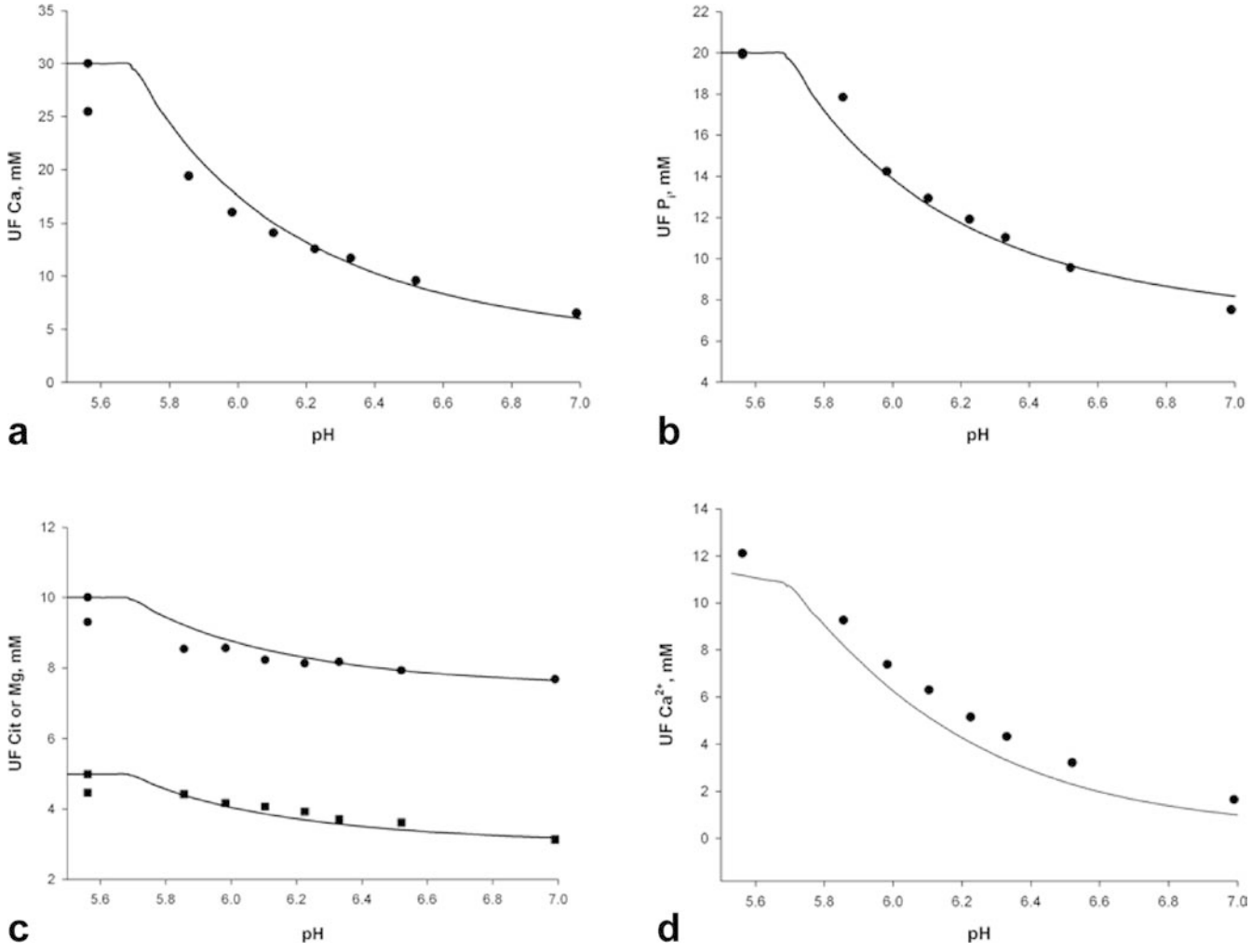

Fig. 5 (**a**) Ca, (**b**) P_i, (**c**) Mg (*squares*), Cit (*circles*) and (**d**) free Ca^{2+} concentrations in UFs of a nanocluster solution in buffer B containing 5 mg β-PP mL^{-1}. The *solid lines* were calculated from a model of the species formed in the solution using $pK_S = 8.0$, $y = 0.4$

The particle scattering factor of a monodisperse core-shell particle exhibits a number of subsidiary maxima as a function of increasing Q outside the Guinier range. The first subsidiary maximum was detected in an earlier neutron scattering experiment, but we have been unable to confirm this observation in numerous experiments by SAXS where the photon counting statistics and monochromicity of the beam are superior and the effect of slit smoothing is less. The smoothing out of subsidiary maxima by polydispersity may be the cause and so an attempt was made to see if the scattering profile could be fitted by a simple model of the polydispersity as represented by Eqs. (28)–(30). A calculated fit to the experimental scattering from the α-PP nanocluster prepared at pH 6.7 is shown in Fig. 4d. Manual searching of the parameter space revealed that there were many close fits and the fitted electron density parameters were so closely correlated that only differences could be determined. Thus, the unweighted best fit by the least-squares criterion, which is shown in Fig. 4d, was for $R_o = 1.08$ nm, $\beta = 0.41$, $(\rho_{shell} - \rho_{core})/\rho_s = -2.24$ and $(\rho_{core} - \rho_s)/\rho_s = 2.59$. Particle scattering factors were very similar over the whole pH range of stability, with the possible exception of the lowest pH where nanoclusters could be detected (5.8–5.9), but here the excess scattering over the solvent is so small that further work will be needed to ensure that the observations are correct.

Effect of pH on the salt composition of nanocluster solution ultrafiltrates

Nanocluster solutions were made with β-PP and either buffer A minus the Mg salt or buffer B, in the pH range 5.5–7.8, and were ultrafiltered. A third series of ultrafiltrations was done on nanocluster solutions prepared using buffer B containing a concentration of 10 mg CPP mL^{-1} over a similar pH range. Although the ultrafiltration membrane had a nominal MWCO of 10,000 Da, the peptides were found to be almost totally impermeable in tests on a model system where all the

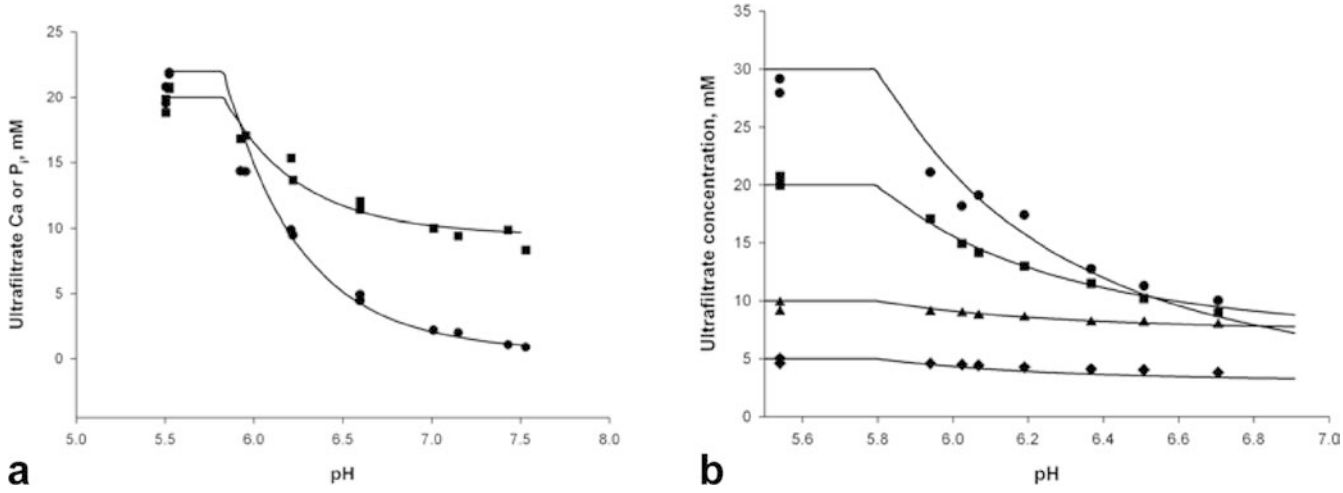

Fig. 6a, b Comparison of experimental UF concentrations of Ca (*circles*), P_i (*squares*), Cit (*triangles*) and Mg (*diamonds*) with predictions of the model (*solid lines*). (**a**) Buffer A without Mg containing 5 mg β-PP mL^{-1}. The calculations used $y = 0.4$ and $pK_S = 7.8$. (**b**) Buffer B with 10 mg CPP mL^{-1}. The calculated lines used $y = 0.4$ and $pK_S = 7.9$

β-PP was free. Typically, more than 90% of the free peptide was retained. The UF salt composition is therefore reduced by the Ca bound to the peptide as well as that present in the form of the nanoclusters. The compositions of the UFs are shown in Figs. 5 and 6. The ion equilibria in the UFs were calculated as previously described (Holt et al. 1981) and the IAP calculated for various values of y in Eq. (9). In Fig. 7, the results of the calculations are given. For each value of y, the IAP values have been divided by their average and a constant added to space out the results in the diagram. Figures 5 and 6 also show the model calculations of the composition of the UFs using the parameters given in the legends. All calculations used $R_{Ca} = 13.2$ and $R_P = 6.5$ and those for buffer B also used $R_{Mg} = 1$ and $R_{Cit} = 1.3$.

For the nanoclusters prepared from buffer A minus Mg with the β-PP, an invariant IAP was obtained for $y = 0.4$ ($Ca/P_i = 1.3$) and $pK_S = 7.8$. For the nanoclusters prepared with buffer B and the β-PP, the very similar values of $y = 0.4$ and $pK_S = 8.0$ were obtained. For the nanoclusters prepared with buffer B and the CPP, the IAP indicated a slightly more acidic core, with $y = 0.6$ ($Ca/P_i = 1.15$) and $pK_S = 7.2$. The pK_S values are, of course, only comparable at the same y, but numerical calculations of the predicted UF compositions were found to be very similar whichever fitted pair of y and pK_S values was used. This is illustrated in Fig. 6b, where an excellent fit to the UF composition of the CPP nanocluster solution was obtained, with parameters typical of the β-PP nanocluster: $y = 0.4$ and $pK_S = 7.9$.

Calculations of the extent of reaction of the β-PP in buffer A minus Mg and buffer B as a function of pH are shown in Fig. 8a. In buffer A there is an excess of unreacted β-PP up to pH 7.5, but in buffer B, all the phosphopeptide has reacted by pH 6.7. Above these points the solution can no longer form the nanoclusters and hence the solution becomes increasingly unstable. The condition of stability in a nanocluster-forming solution can be expressed as:

$$\alpha = \frac{[P_i]_c}{[\beta - PP]R_P} \leqslant 1 \qquad (31)$$

The calculation of the extent of reaction in the nanocluster solutions formed from CPP requires further information on how the peptides in the CPP participate in forming nanoclusters than is presently available. In Fig. 8b the apparent IAP in the β-PP–buffer B solution is shown over a wider range of pH values than in Fig. 7c. Linear regression lines fitted separately to points above and below pH 6.7 show a change of slope at about this point and the invariant IAP in the more alkaline pH range corresponds to a more basic salt, with $y \leq 0.1$.

The experiments shown in Fig. 3 were all performed at pH≈6.7 and the buffers had very similar UF P_i concentrations. In other words, at a peptide concentration of 1.6 mM, $\alpha \approx 0.9$, as calculated in Fig. 8a, but at the higher peptide concentrations shown in Fig. 3a, α is smaller so that, for example, at 6.4 mM β-PP the concentration of free peptide is nearly 5 mM ($\alpha = 0.78$).

The experiments shown in Fig. 4a and Fig. 4b show an increase in the radius of gyration of the nanocluster solution above pH 7.5. The effect is explained quite economically by the exhaustion of free peptide in the formation of nanoclusters at the lower pH and the formation of larger colloidal particles at the more alkaline pH values.

Dispersion of precipitated calcium phosphate

Figure 9 shows the effect of time and CPP concentration on the dispersion of a fresh precipitate of amorphous calcium phosphate. At 2 mg mL^{-1} the CPP caused the precipitate to swell to a maximum volume fraction just above 0.5 after 40–50 days and to decline thereafter, while the turbidity in the continuous phase gradually increased. At 5 mg mL^{-1} the precipitate volume swelled

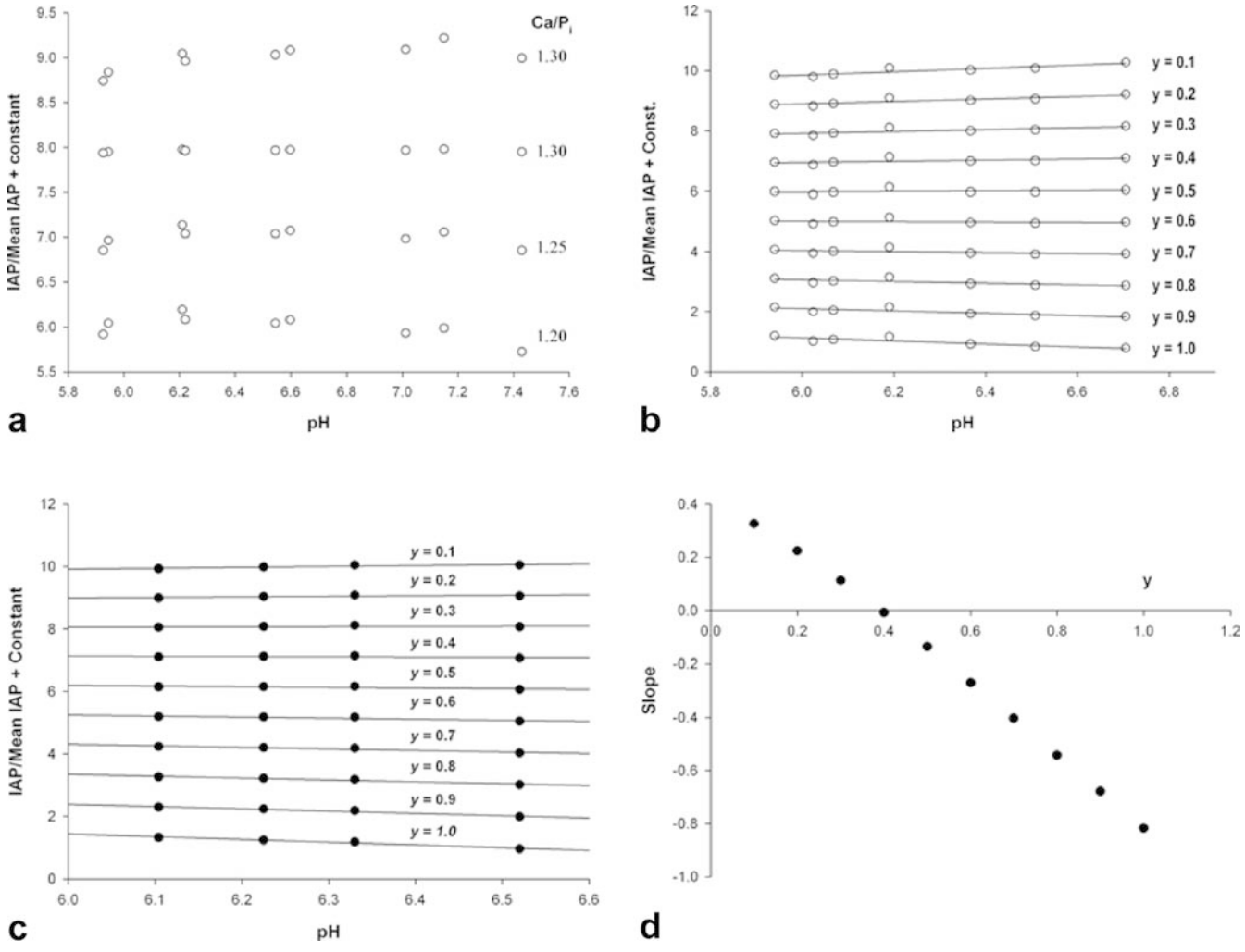

Fig. 7 Calculation of ion activity products corresponding to different y values in UFs of nanocluster solutions prepared with (**a**) buffer A minus Mg and β-PP, (**b**) buffer B and CPP and (**c**) buffer B and β-PP. In (**d**) the slope of the linear regression line for the results in Fig. 7c is shown to pass through zero at $y = 0.4$, giving the form of the invariant constant

to form a turbid gel, occupying the whole volume after about 30 days; the gel then clarified and exhibited a limited degree of syneresis. The fastest rate of clarification was found at 10 mg mL^{-1} and an intermediate gel phase was not observed, but the higher concentration of 20 mg mL^{-1} did not produce a further increase in the rate of dispersal of the precipitate. After 3 months, there did not appear to be any further change in the appearance of the contents of the bottles and the clear supernatants were examined by SAXS at 3, 6 and 9 months. All the supernatants contained particles that were, on average, too large to be studied in the Guinier region, but the sizes appeared to be decreasing slowly with time towards typical CPN values.

The dissolution was also observed of precipitates formed from buffer B. Subsequent additions were made of 5, 10 and 20 mg β-PP mL^{-1}. The rate appeared faster than with the CPP and to be proportional to the peptide concentration; no intermediate gel state was seen and dissolution went to completion at all three concentrations. Neither CPP nor β-PP was able to disperse a calcium phosphate precipitate prepared from buffer A or crystalline DCPD within 6 months. Thus, although CPN complexes can be prepared without Cit or Mg by the forward reaction, the rate of dispersion of the Cit-free ACP by the phosphopeptides was much slower.

Thus, the ACP containing Cit appeared to disperse more readily and rapidly, indicating that it may have ripened into a more thermodynamically stable state than the ACP without Cit by the time the phosphopeptide was added. Fresh precipitates prepared from buffers A and B were immediately frozen and freeze-dried and examined by X-ray powder diffraction. Although there were some small differences between the samples in the shape of the broad envelope of scattering, neither showed the sharp diffraction lines of a crystalline material and both would be classified as essentially amorphous (results not shown).

Nanocluster solutions at the usual pH of 6.7 may be frozen and thawed with no change in their appearance. However, when a series of nanocluster solutions was prepared in buffer B at a β-PP concentration of

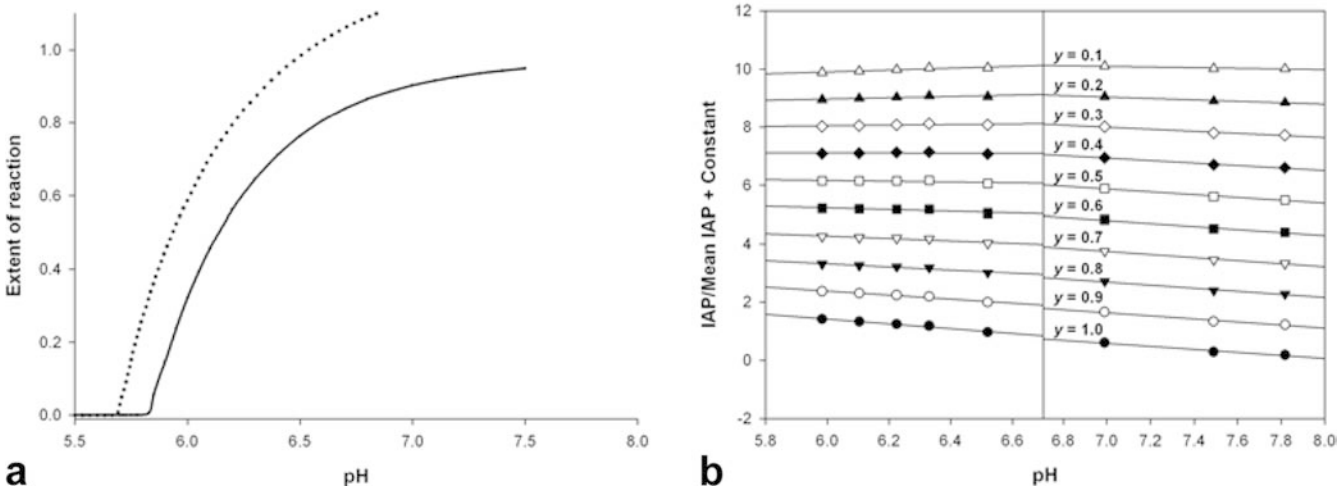

Fig. 8 (**a**) Extent of reaction of the β-PP at 1.6 mM in buffer A minus Mg (*solid line*) and buffer B (*dotted line*) as a function of pH. (**b**) IAP calculations for the β-PP nanocluster solutions in buffer B. Linear regression equations were fitted to the two sets of results above (pH > 6.7) and below (pH < 6.7) $\alpha = 1$

10 mg mL^{-1} in the pH range 6–7.8, then frozen at −20 °C for two weeks and thawed, a precipitate of calcium phosphate formed in the more alkaline solutions, even though it was calculated that there was an excess of the β-PP over that needed to form the nanoclusters over the entire pH range. However, the precipitate gradually dissolved on standing at room temperature over a period of several weeks.

Conclusions

Evidence has been presented that the calcium phosphate nanocluster is an equilibrium complex. The previous understanding of the nature of CPN was based on a model of arrested precipitation in which they had kinetic but not thermodynamic stability. This has now been shown to be incorrect since nanocluster-like particles can be formed, albeit slowly, by the reverse reaction starting from an amorphous calcium phosphate precipitate.

Amorphous calcium phosphate precipitates prepared in the absence of phosphopeptide have a relatively constant composition above pH 7.4, with the formula $Ca_3(HPO_4)_{0.2}(PO_4)_{1.87}$ (Mayer and Eanes 1978), corresponding to $y = 0.066'$, Ca/P = 1.45 and $pK_{Sp} = 8.3$ in Eq. (9). However, at lower pH the proportion of HPO_4^{2-} increases and Ca/P values as low as 1.15 have been found (Wuthier et al. 1985; Holt et al. 1988), corresponding to $y = 0.6$, but the amorphous phase is very unstable. The core composition of the nanoclusters, as indicated by the y value of 0.4, has 50% of the P_i in a protonated form, but, unlike the bulk phase, it appears to be stable. The amorphous phase has no long-range crystalline order and, as a result, no lattice energy. Indeed, it may be necessary for the core of a nanocluster to be amorphous if the free energy of sequestration of the core particle is to bring the overall free energy below that of the formation of the bulk phase, as required in Eq. (15).

In general, the structural requirements for calcium phosphate sequestration by caseins are incompletely known. The present results suggest that an equilibrium is formed by balancing a forward reaction of the growth of an ACP precipitate against a back reaction which involves the substitution of the peptide phosphate centre into the surface of a growing ACP nucleus. It has been observed that the preparation of metastable ACPs (i.e. ones that do not quickly mature into a crystalline phase) at a pH as low as 6 is facilitated by the presence of Cit and Mg (Holt et al. 1989) and that these ACPs contain a high proportion of the P_i as HPO_4^{2-} ions. Holt and Hukins (1991) suggested that since the phosphate moiety of phosphoserine and the HPO_4^{2-} ion have essentially C_{3v} symmetry, are isoelectric, isolobal and have the same H-bonding capability, the interaction of phosphopeptides with acidic ACPs is particularly favourable. Moreover, in sequestering the calcium phosphate, the whole phosphate centre can be regarded as a multidentate ligand, able to compete well with single P_i ions because the binding of the phosphate centre generates an increase in the number of degrees of freedom of the system through the displaced water molecules (the chelate effect). Structural factors that might influence the point of equilibrium will most likely include primarily the size and structure of the phosphate centre, but, to a lesser degree, the length, conformation and chemical nature of the rest of the polypeptide chain may be important in providing a steric limit to how small the CPN can be in circumstances where the chelate effect is strong.

Because the CPN forms an equilibrium distribution of sizes when the peptide is in excess, it seems most unlikely that the size of the nanocluster is uniquely determined by any symmetry constraint on the packing of peptides in the shell, in contrast, for example, to many

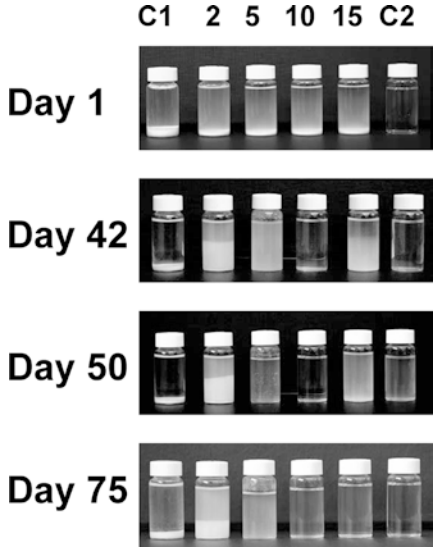

Fig. 9 Effect of the concentration of CPP on the dispersion of a freshly prepared precipitate of amorphous calcium phosphate. *From left to right*, the concentrations of CPP were 0 (control 1), 2, 5, 10, 20 and 20 (control 2) mg mL^{-1}. The precipitates were formed by raising the pH from 5.5 to 6.7 of buffer B and then adding the peptide after 30 min of equilibration. Control 2 did not contain any P_i, and hence did not form a precipitate

virus protein envelopes. The equilibrium state is insensitive to many of the solution conditions under which it is formed. Thus, nanoclusters of a given average size and composition are formed independently of (1) the phosphopeptide concentration, provided it is above the minimum ($\alpha \leq 1$), (2) temperature, (3) pH, (4) Mg and Cit concentrations and (5) time. In practice, therefore, it is possible to represent the nanocluster as a unique complex with the average size and composition of the distribution and to calculate the remaining chemical species present in the solution. It remains to be demonstrated whether the parameters needed for these calculations (K_S, y, R_{Ca} and R_P) are independent of the nature of the phosphate centre. Within the paralogous group of SCPPs, none other than caseins has so far been described as having a calcium phosphate sequestration function, although many do bind to the calcium phosphate of bone, dentine and enamel. Nonetheless, β-casein is an archetypal member of the group, having an N-terminal phosphate centre, a Pro-rich linker sequence and a C-terminal recognition or non-specific binding domain, so it seems likely that the ability to sequester as well as bind calcium phosphate will be found in other members of the group.

Acknowledgements We thank Günter Grossmann (CCLRC Daresbury Laboratory), Xiaolin Qi, Deborah McPhail, Sally Taylor, Julie Currie and Ed Smyth (all HRI) for their help with the SAXS measurements. Jeff Leaver at HRI and Garry Woffendin and Michaela Scigelova of ThermoFinnigan Applications Laboratory, Milton Keynes, UK are thanked for the mass spectral analyses on the α-PP. Roger Clegg (HRI) and Ed Smyth offered useful critical comments on the manuscript. The work was supported financially by the UK BBSRC and SEERAD.

References

Allan RJL (1940) The estimation of phosphorus. Biochem J 34:858–865

Baumy JJ, Guenot P, Sinbandhit S, Brulé (1989) Study of calcium binding to phosphoserine residues of β-casein and its phosphopeptide (1–25) by ^{31}P NMR. J Dairy Res 56:403–409

Connerty HV, Briggs AR (1966) Determination of serum calcium by means of orthocresolphthalein complexone. J Clin Pathol 45:290–296

De Kruif CG, Holt C (2003) Structure, functions and interactions of casein micelles, In: Fox PF, McSweeney P (eds), Advanced dairy chemistry, vol 1: proteins, 3rd edn. Kluwer/Plenum, New York, pp 233–276

Dunker AK, Brown CJ, Lawson JD, Iakoucheva LM, Obradovic Z (2002) Intrinsic disorder and protein function. Biochemistry 41:6573–6582

Dyson HJ, Wright PE (2002) Coupling of folding and binding for unstructured proteins. Curr Opin Struct Biol 12:54–60

Ellegård KH, Gammelgård-Larsen C, Sørensen ES, Fedosov S (1999) Process scale chromatographic isolation, characterization and identification of tryptic bioactive casein phosphopeptides. Int Dairy J 9:639–652

Feigin LA, Svergun DI (1987) Structural analysis by small-angle X-ray and neutron scattering. Plenum, New York

Fisher LW, Fedarko NS (2003) Six genes expressed in bones and teeth encode the current members of the SIBLING family of proteins. Conn Tiss Res 44(Suppl 1):33–40

Holt C (2000) Calcium phosphate nanoclusters and their applications. UK Pat GB 2,359,305B (priority date 15 December 1999)

Holt C, Hukins DWL (1991) Structural analysis of the environment of calcium ions in crystalline and amorphous calcium phosphates by X-ray absorption spectroscopy and a hypothesis concerning the biological function of the casein micelle. Int Dairy J 1:151–165

Holt C, Sawyer L (1993) Caseins as rheomorphic proteins: interpretation of primary and secondary structures of the α_{S1}-, β- and κ-caseins. J Chem Soc Faraday Trans 89:2683–2692

Holt C, Dalgleish DG, Jenness R (1981) Calculation of the ion equilibria in milk diffusate and comparison with experiment. Anal Biochem 113:154–163

Holt C, van Kemenade MJJM, Harries JE, Nelson LS Jr, Bailey RT, Hukins DWL, Hasnain SS, de Bruyn PL (1988) Preparation of amorphous calcium phosphates at pH 7 and characterisation by X-ray absorption and Fourier transform infrared spectroscopy. J Cryst Growth 92:239–252

Holt C, van Kemenade MJJM, Nelson LS Jr, Harries JE, Bailey RT, Hukins DWL, Hasnain SS, de Bruyn PL (1989) Amorphous calcium phosphates precipitated at pH 6.5 and 6.0. Mater Res Bull 23: 55–62

Holt C, Wahlgren NM, Drakenberg T (1996) Ability of a β-casein phosphopeptide to modulate the precipitation of calcium phosphate by forming amorphous dicalcium phosphate nanoclusters. Biochem J 314:1035–1039

Holt C, Timmins PA, Errington N, Leaver J (1998) A core-shell model of calcium phosphate nanoclusters derived from sedimentation equilibrium and small angle X-ray and neutron scattering measurements. Eur J Biochem 252:73–78

Holt C, de Kruif CG, Tuinier R, Timmins PE (2003) Substructure of bovine casein micelles by small-angle X-ray and neutron scattering. Colloids Surf 213:275–284

Kawasaki K, Weiss KM (2003) Mineralized tissue and vertebrate evolution: the secretory calcium-binding phosphoprotein gene cluster. Proc Natl Acad Sci USA 100:4060–4065

Mayer JL, Eanes ED (1978) A thermodynamic analysis of the amorphous to crystalline calcium phosphate transition. Calcif Tiss Res 25:59–68

McMeekin TL (1971) Milk proteins in retrospect. In: McKenzie HA (ed) Milk proteins chemistry and molecular biology, vol 1. Academic Press, New York, pp xxx–xxx

Petrescu A-J, Receveur V, Calmettes P, Durand D, Smith JC (1998) Excluded volume in the configurational distribution of a strongly-denatured protein. Protein Sci 7:1396–1403

Qi XL, Holt, C, McNulty D, Clarke DT, Brownlow S, Jones GR (1997) Effect of temperature on the secondary structure of ß-lactoglobulin at pH 6.7, as determined by circular dichroism and infrared spectroscopy: a test of the molten globule hypothesis. Biochem J 324:341–346

Rijnkels M (2002) Multispecies comparison of the casein gene loci and evolution of casein gene family. J Mammary Gland Biol Neoplasia 7:327–345

Syme CD, Blanch EW, Holt C, Goedert M, Hecht L, Barron LD (2002) A Raman optical activity study of rheomorphism in caseins, synucleins and tau: new insight into the structure and behaviour of natively unfolded proteins. Eur J Biochem 269:148–156

Tompa P (2002) Intrinsically unstructured proteins. Trends Biochem Sci 27:527–533

Towns-Andrews E, Berry A, Bordas J, Mant GR, Murray PK, Roberts K, Summer I, Wogan JS, Lewis R (1989) Time resolved X-ray diffraction station: X-ray optics, detectors and data acquisition. Rev Sci Instrum 60:2346–2349

Wuthier RE, Rice GS, Wallace JEB Jr, Weaver RL, LeGeros RZ, Eanes ED (1985) In vitro precipitation of calcium phosphate under intracellular conditions: formation of brushite from an amorphous precursor in the absence of ATP. Calcif Tiss Int 37:401–410